applied sciences

MDPI

Article

Fast Method of Computations of Ripples in the Junction Temperature of Discrete Power SiC-MOSFETs at the Steady State

Krzysztof Górecki * and Paweł Górecki

Department of Marine Electronics, Gdynia Maritime University, Morska 81-87, 81-225 Gdynia, Poland
* Correspondence: k.gorecki@we.umg.edu.pl

Featured Application: The presented results can be applied in computer analyses of switched networks and in the proper estimation of the junction temperature of transistors in such networks.

Abstract: This paper presents a method of fast computations of waveforms of the junction temperature of power SiC-MOSFETs (silicon carbide metal–oxide–semiconductor field-effect transistor) operating in switched-mode circuits at the steady state. This method makes it possible to use SPICE (Simulation Program with Integrated Circuits Emphasis) models of the considered transistors given by the manufacturers. The method of the analysis is described. Using the presented methods and a compact thermal model, some computations of switch-mode circuits were performed. Typical switches and DC–DC (direct current to direct current) boost converters, including such transistors operating at different cooling conditions in a wide range of frequencies of a control signal, are analyzed. In particular, the influence of the cooling system, load resistance and switching frequency on the waveforms of the dissipated power and the junction temperature are considered. The obtained results of computations are compared with the results found using other methods of analysis given in the literature. The times required to perform computations with the considered methods are compared. On the basis of the results of the performed analyses, the operating conditions of the investigated networks, at which ripples of the junction temperature are important, are pointed out. A short discussion on the limitation of the lifetime of the power MOSFET is also given.

Keywords: power SiC-MOSFETs; junction temperature; self-heating; SPICE; electrothermal analysis; switched networks; DC–DC converters; computation method

Citation: Górecki, K.; Górecki, P. Fast Method of Computations of Ripples in the Junction Temperature of Discrete Power SiC-MOSFETs at the Steady State. *Appl. Sci.* **2022**, *12*, 8887. https://doi.org/10.3390/app12178887

Academic Editors: Zbigniew Kaczmarczyk, Pooya Davari and Zbigniew Rymarski

Received: 12 August 2022
Accepted: 2 September 2022
Published: 5 September 2022

1. Introduction

Power semiconductor devices, particularly power transistors, are commonly used in switching circuits [1–3]. In these systems, the power p dissipated in transistors changes strongly as a function of time, and the junction temperature T_j can significantly exceed the value of the ambient temperature T_a as a result of the self-heating phenomenon [4–6]. In order to correctly compute the waveforms of the power $p(t)$ and junction temperature $T_j(t)$, it is necessary to perform electrothermal analyses using electrothermal models [7–9]. The models mentioned above take into account the influence of mutual interactions between the temperature T_j and the voltages and currents of the transistor [10–12].

In electrothermal models, compact thermal models describing the dependence of the junction temperature on the dissipated power p are often used. Transient thermal impedance $Z_{th}(t)$ is the parameter characterizing the heating process of a transistor in a specific cooling system [13–15]. In this study transient thermal impedance, junction–ambient, is considered. The course of $Z_{th}(t)$ is typically described using the sum of the exponential functions [7,16,17]

$$Z_{th}(t) = R_{th} \cdot \left[1 - \sum_{i=1}^{N} a_i \cdot \exp\left(-\frac{t}{\tau_{thi}}\right)\right] \quad (1)$$

where R_{th} is thermal resistance, a_i is the weight coefficients related to thermal time constants τ_{thi} and N is the number of thermal time constants.

In Formula (1), there are thermal time constants τ_{thi} characterizing individual components of the heat flow path, and their values differ from each other by several orders of magnitude [17,18]. In the electrothermal analysis of switching circuits, there is a problem of how to solve the system of differential-algebraic equations, in which there are significant differences between the values of the time constants characterizing the electrical and thermal properties of the analyzed circuit. The differences between these time constants can reach nine orders of magnitude [4,19], which causes an unacceptable increase in the duration time of the calculations necessary to obtain the steady state. Therefore, many methods have been developed that make it possible to shorten this time by applying various simplifications. Many of these methods are characterized in the paper [4].

For example, the use of the so-called electrothermal averaged models [20] allows the performance of fast analyses with the omission of time changes in the power dissipated in semiconductor devices. In the analyses carried out with these models, it is not possible to accurately determine the peak-to-peak value of ripples of the junction temperature T_j; only its average value can be determined. When using the accelerated transients analysis [4], the influence of the shortest and longest thermal time constants on the determined waveforms $T_j(t)$ is ignored. Therefore, the results of such calculations are not precise.

In the paper [19] an iterative method of electrothermal transient analysis of DC–DC converters is proposed, in which the calculations are performed iteratively with the use of SPICE and a program extrapolating the values of voltages, currents and junction temperatures with the use of memoryless convolution algorithms [21]. This method does not require simplifications, but its practical application requires the preparation of a special program.

Modern constructions of power transistors are characterized by a method of mounting a semiconductor die to the metal base, which causes the occurrence of thermal time constants in the transient thermal impedance of the transistor of a much lower value, even up to a dozen microseconds [22]. This may cause the occurrence of thermal cycles, which adversely affects the reliability of the considered class of transistors [23,24].

On the other hand, the typical values of the control signal period are much shorter than the thermal time constants for classic power transistors [4,25]. Therefore, in the computer analyses of switching circuits with these transistors, ripples of the junction temperature are typically neglected at the steady state [4,26].

Now, more and more popular power semiconductor devices are made of wide bandgap semiconductor materials [27–30]. In this group the devices made of silicon carbide (SiC) play an important role. Such devices are characterized by a high value of the maximum allowable voltage and high switching frequency [28]. In the papers [27–30] much information is given regarding the possibility of replacing silicon power transistors with such devices made of silicon carbide.

In this paper, a fast computation method of ripples in the junction temperature of discrete power SiC-MOSFETs at the steady state is proposed. This method is applied based on the concept described in [19] but is possible to be implemented by the method of separated iterations with the SPICE software, without the need to use other programs. The elaborated method is described and the method of its practical implementation in the SPICE software is presented on the example of a power SiC-MOSFET. The usefulness of the proposed method is shown for two circuits: a transistor switch and a boost converter. Some results illustrating the influence of the cooling conditions of the tested transistor, switching frequency and load resistance on the waveforms of the power dissipated in this transistor and its junction temperature are shown and discussed. The investigations were performed for three different cooling systems of the tested transistor.

Section 2 presents the proposed calculation method and the manner of its implementation in SPICE. Section 3 contains a description of the analyzed circuits and the considered

cooling conditions of the tested transistors. Section 4 presents and discusses the obtained results of the calculations.

2. Computation Method

The methods of electrothermal analyses of electronic networks with the use of SPICE need a special electrothermal model implemented in this software. On the other hand, the manufacturers give on their websites the models of their products dedicated for SPICE. Such models are in the form of subcircuits and they do not take into account the self-heating phenomenon. The proposed computation method makes it possible to use such models in computations and obtain a much shorter time of computations.

This method includes the six steps:

(a) Setting the value of the transistor temperature TEMP equal to ambient temperature T_a.
(b) Transient analysis of the tested circuit for a time equal to two periods of the control signal and registrations of the waveforms of $p(t)$ and $T_j(t)$.
(c) Calculation of the average value of power p_{avg} dissipated in the transistor using the results of the SPICE computations.
(d) Calculation of the junction temperature T_j value at the steady state using the formula

$$T_j = T_a + R_{th} \cdot p_{avg} \tag{2}$$

(e) Comparing the values of TEMP and T_j. If the difference is bigger than 1 K, TEMP should be substituted by T_j and then jump to point (b). If this condition is not fulfilled, jump to point (f).
(f) Waveforms of $p(t)$ and $T_j(t)$ obtained in point (b) correspond to the waveforms of these quantities at the steady state.

Practical implementation of the proposed method is presented below on the example of a power SiC-MOSFET offered by ROHM semiconductor [31]. The network representation of the model of the considered transistor is presented in Figure 1.

In this model, terminals D, G and S represent drain, gate and source of the modeled transistor, respectively. Controlled current sources G1 and G11 describe DC components of the drain current. Voltage sources V1, V2, V3, V11 and V12 of zero values are used to monitor the current flowing through selected branches and used in the description of selected controlled sources. Resistors R3 and R11 have very high values and they are used due to the formal requirements of the SPICE software. Linear capacitors C11, C1 and C2 and controlled current sources G2 and G11 represent internal capacitances of the transistor. Inductor L1 describes the inductance of the source. The output voltages or currents of the following controlled voltage and current sources E3, E4, E1, G1 and G11 depend on temperature TEMP. Controlled voltage sources E1 and E2 describe series resistances of the gate and the drain taking into account an influence of temperature. Controlled voltage source E11 describes non-linear series resistance of the source. Controlled voltage sources E3 and E4 are used to calculate the formulas used in the descriptions of other currents or voltages sources contained in this model. Many of the used controlled voltage and current sources are described using splines.

In order to perform computations with the use of the proposed method in SPICE, an input file should be included with the schema of the analyzed network with the transistor model presented in Figure 1 and the network representation of its thermal model in the form shown in Figure 2. In this network-controlled current source, p_{th} represents power dissipated in the transistor, which is equal to the product of drain current i_D and voltage between the drain and the source v_{DS}. Resistors occurring in this network represent thermal resistance of each component of the heat flow path, whereas capacitors represent thermal capacitances of these components. Values of these resistors are equal to the product of thermal resistance R_{th} and coefficients a_i, whereas thermal time constants τ_{thi} are equal to the products of thermal capacitances C_{thi} and thermal resistances R_{thi}. Of course, the number of components R_{thi} and C_{thi} as well as their values depend on properties of the

used cooling system of the tested transistor. Voltage ΔT_j on controlled current source p_{th} corresponds to an excess of the transistor junction temperature over the ambient one.

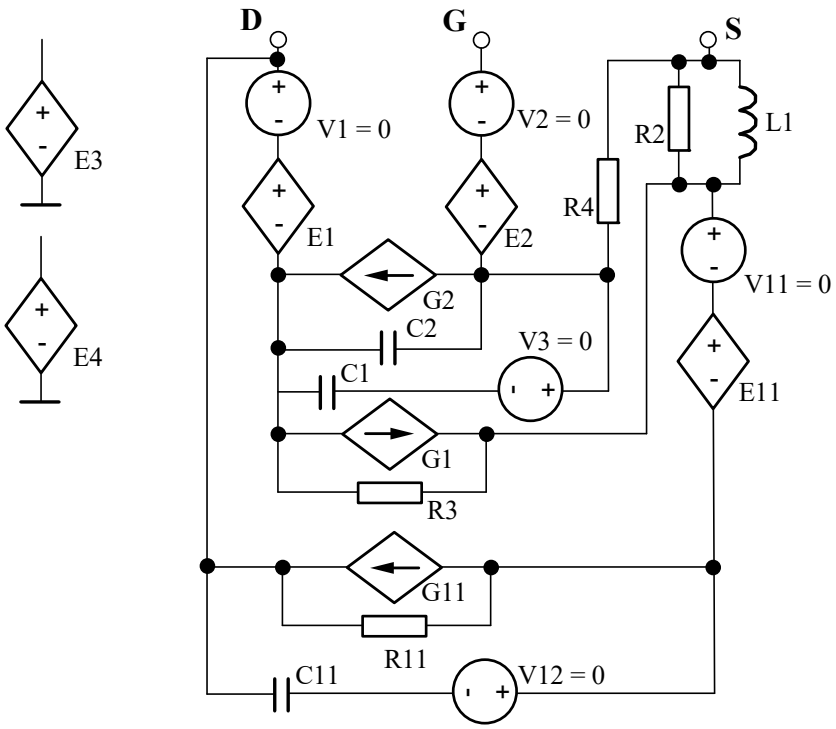

Figure 1. Network representation of the model of a SiC-MOSFET given in [32].

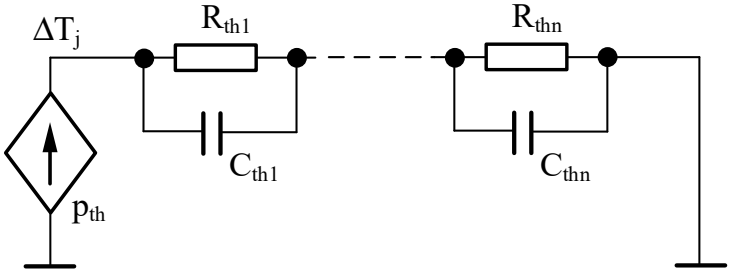

Figure 2. Network representation of the used thermal model of a SiC-MOSFET.

In the practical analyses the following steps should be performed in order to obtain the waveform of the transistor junction temperature:

1. At first, a SPICE input file should be formulated. In this file the option TEMP should be equal to the ambient temperature given in Celsius degrees and the initial conditions of capacitors' voltages in the thermal model should be equal to zero.
2. Next, the transient analysis of the tested network is performed with the final time equal to two periods of a stimulating signal.
3. After this analysis, the average value p_{avg} of the power dissipated and the peak-to-peak value T_{jpp} of ΔT_j are calculated using a graphical post-processor of SPICE for the time equal to the doubled period of the stimulating signal.
4. Next, the average value T_{javg} of the transistor junction temperature at the steady state is estimated using the Formula (2).
5. If the value of TEMP differs from the difference $T_{javg} - T_{jpp}/2$ more than 1 °C, the algorithm should jump to point 6, otherwise, the results obtained in point 2 correspond to the steady state and the algorithm stops.
6. The SPICE input file is modified. In this file the value of TEMP equal to the difference between T_{javg} and $T_{jpp}/2$ is set and the algorithm jumps to point 1.

3. Investigated Circuits

Two circuits are selected for the tests of the usefulness of the elaborated algorithm. The first is a power MOSFET switch, the diagram of which is shown in Figure 3a, and the other is a boost converter, the diagram of which is shown in Figure 3b.

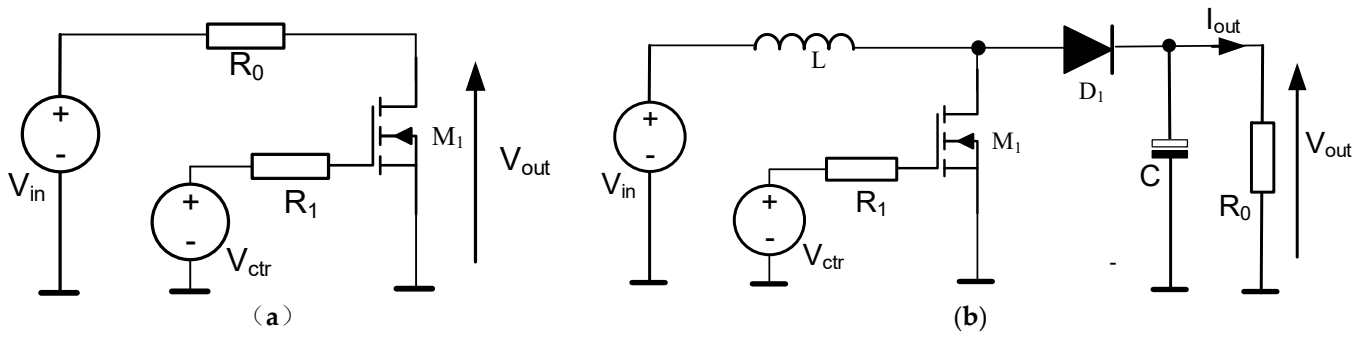

Figure 3. Diagrams of the investigated circuits: (**a**) transistor switch, (**b**) boost converter.

In both the considered circuits, a SiC-MOSFET transistor of the SCT3060AL type is used. This transistor is characterized by the maximum allowable value of the voltage between the drain and the source equal to 650 V, the maximum allowable drain current value of 39 A and the resistance of the switched on channel R_{ON} = 60 mΩ [31]. In the practical application, such a transistor can be driven using monolithic drivers, e.g., offered by Infineon Technologies. One of the possible solutions is the driver IR2125 [33].

Voltage source V_{in} supplies the tested circuits with DC voltage, resistor R_0 is the load of the circuits, voltage source V_{ctr} generates the signal that drives the transistor gate with the shape of a rectangular pulse train with frequency f, the duty cycle d = 0.5 and voltage levels equal 0 and 15 V, respectively. Resistor R_1 limits the value of the transistor's gate current. Diode D_1 is an impulse diode, capacitor C has the capacitance of 1 mF and inductor L has the inductance of 1 mH.

The voltage value V_{in} = 200 V and the resistance of resistor R_1 = 30 Ω are assumed in the calculations. Different values of load resistance R_0 and three types of cooling conditions of the tested transistor are considered, corresponding to:

(a) a transistor operating without an additional cooling system (system A),
(b) a transistor mounted in a system containing a heat sink and a fan (system B),
(c) a transistor mounted in the cooling system ensuring perfect cooling of its case: the ideal cold plate (system C).

Table 1 shows the values of the thermal model parameters for the three considered cooling systems.

The cooling conditions described above are characterized at the steady state by thermal resistance R_{th}, the values of which are, respectively, equal to: 42.5 K/W, 3.2 K/W and 0.7 K/W [31,34]. The waveforms of the transient thermal impedance $Z_{th}(t)$ of the transistor operating under the above-mentioned cooling conditions, normalized to the value of thermal resistance, are shown in Figure 4.

This figure shows that the time required to achieve the steady state strongly depends on the cooling system. This time is the longest for system B (1500 s) and the shortest for system C (20 ms). In the description of $Z_{th}(t)$ under consideration, there are from 3 to 5 thermal time constants corresponding to a_i coefficients not lower than 0.01. The shortest of these are equal to 0.8 s for system A, 0.1 ms for system B and 0.4 ms for system C.

Table 1. Values of parameters of the considered cooling systems.

Parameter	System A	System B	System C
R_{th} (K/W)	42.5	3.2	0.7
a_1	0.04	0.03	0.2
τ_{th1} (s)	0.8	0.0001	0.0004
a_2	0.86	0.07	0.15
τ_{th2} (s)	42	0.01	0.0045
a_3	0.1	0.5	0.65
τ_{th3} (s)	105	0.7	0.006
a_4		0.05	
τ_{th4} (s)		8	
a_5		0.35	
τ_{th5} (s)		540	

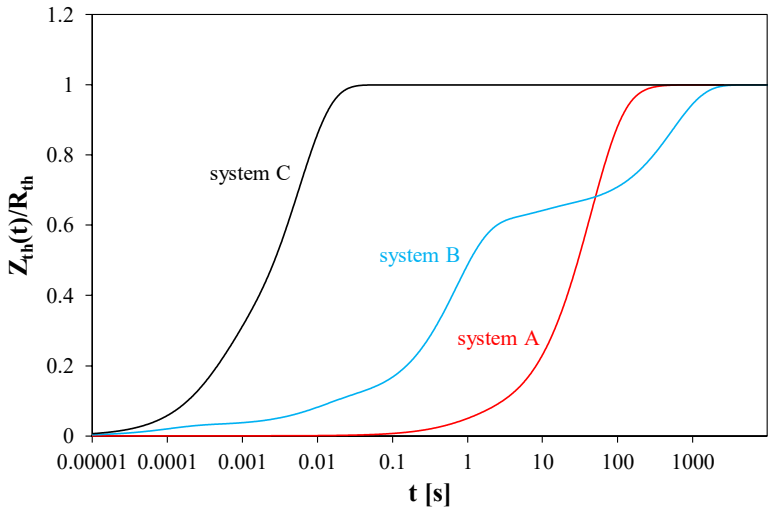

Figure 4. Transient thermal impedance waveforms normalized to thermal resistance for the considered cooling systems.

4. Investigations Results

Using the analysis method described in Section 2, the computations of both the circuits shown in Figure 3 were carried out for all the considered transistor cooling systems. The calculations adopted the diode model embedded in SPICE, and the values of its parameters are as follows: IS = 1 pA, N = 1, CJO = 30 pF. Due to the significant differences in the values of thermal resistance for individual cooling systems, the range of the calculations was limited to the operating conditions, where the excess of the junction temperature of the transistor over the ambient temperature at the steady state does not exceed 200 K. The values of switching frequency f were also limited to the range from 1 to 400 kHz.

In Section 4.1 the comparison of the results performed with the use of the new method and a selected method given in the literature are presented. Next, in Section 4.2 the influence of properties of the used cooling system and the operation range of the tested networks are presented.

4.1. Verification of the Method

In order to prove the correctness of the proposed computation method (new method), the results obtained with this method were compared with the results obtained with the classical method of transient analysis and the method using one non-physical thermal time

constant (one tau method) [4]. In the one tau method, only one thermal time constant equal to 5 ms is used. The verification of the proposed method is performed for the switch operating with R_0 = 4.5 Ω cooling system C and three values of frequency equal to 1 kHz, 10 kHz and 100 kHz, respectively. This cooling system is selected for such investigations because it is characterized by the shortest time needed to obtain the steady state. Due to such thermal properties of the tested transistor, the biggest changes in the junction temperature are expected. For other cooling systems, such changes should be smaller. The obtained results of the computations are given in Figure 5. In this figure the results obtained using the new method are marked with red, using the classical method of transient analysis, with blue, and using the one tau method, with black.

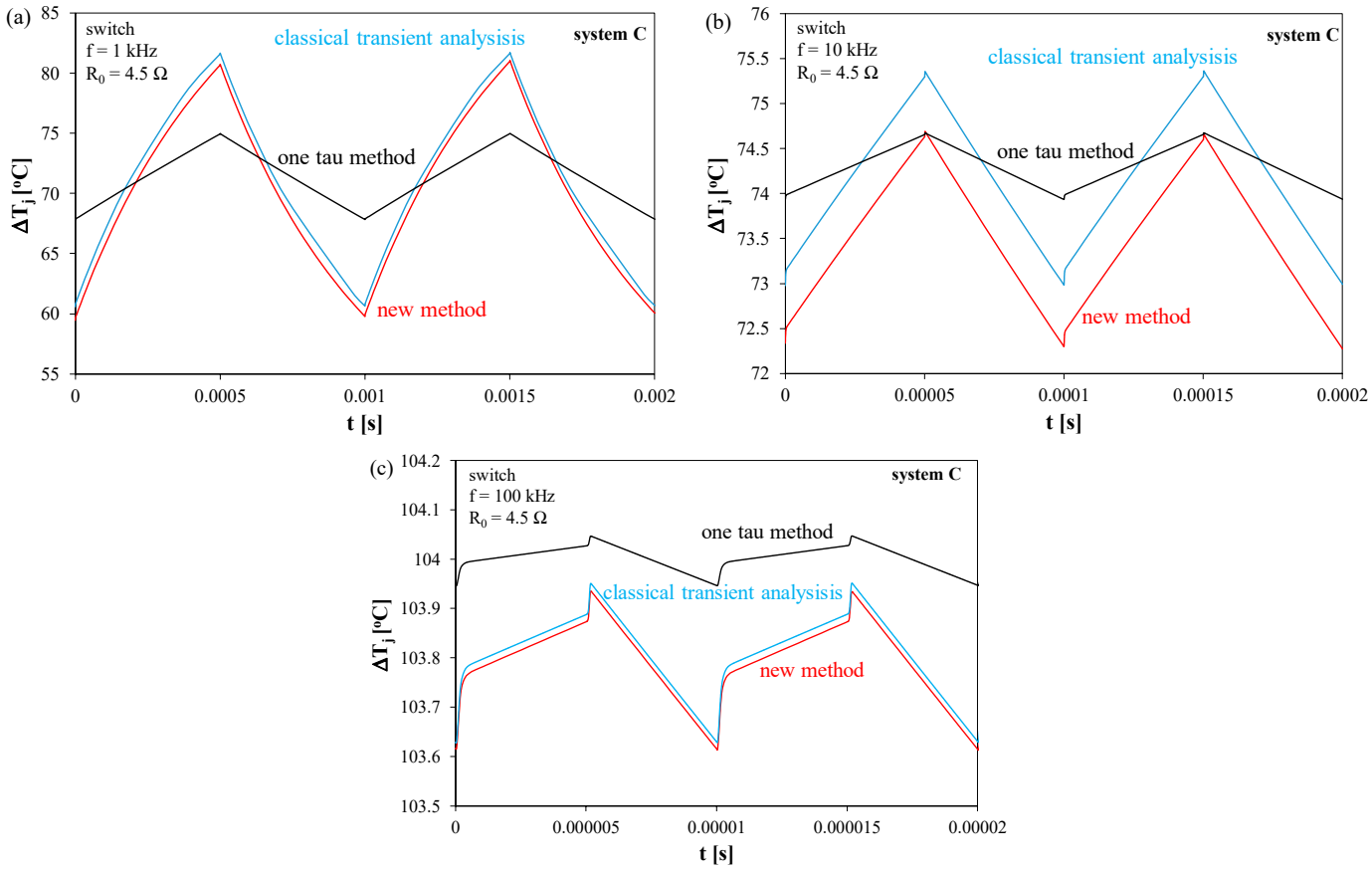

Figure 5. Computed waveforms of the junction temperature of the transistor operating as a switch with the cooling system C at frequency f equal to 1 kHz (**a**), 10 kHz (**b**) and 100 kHz (**c**).

As can be observed, the results obtained with the use the new method and the classical transient analysis are very close to each other. The differences between these results do not exceed 1 °C and the peak-to-peak values obtained with these methods are practically the same. In contrast, the results obtained with the one tau method are characterized by the same average value as the other considered methods, but the peak-to-peak values of the obtained waveforms are more than two times lower than for the other methods. It is also worth observing that an increase in the switching frequency from 1 to 100 kHz causes a visible decrease (over 20 times) in the peak-to-peak value of the considered temperature and an increase in the average value of this temperature. The presented results prove the usefulness of the proposed method. The calculation time for the new method is five times shorter than for the classical method at a frequency equal to 1 kHz. The computation time of the new method does not depend on the frequency and values of thermal time constants. In contrast, this time, while using the classical method, increases nearly linearly with an increase in the values of the longest thermal time constant and switching frequency.

In order to illustrate the usefulness of the proposed method for different values of load resistance, some computations were repeated for a load resistance equal to 10 Ω. The results of such computations obtained at a frequency equal to 1 kHz and 100 kHz are shown in Figure 6.

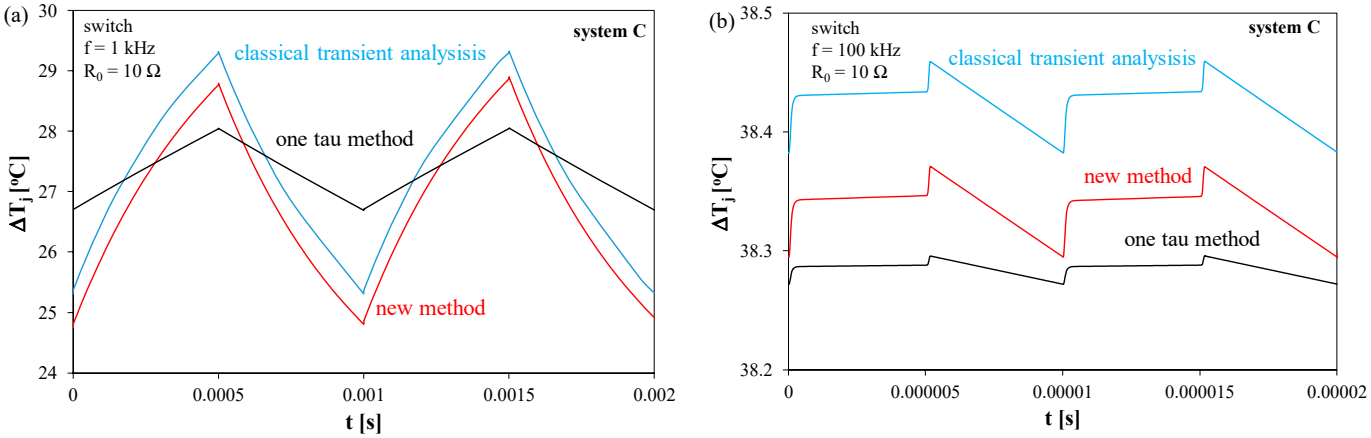

Figure 6. Computed waveforms of the junction temperature of the transistor operating as a switch with the cooling system C at frequency f equal to 1 kHz (**a**) and 100 kHz (**b**).

As is visible, a good agreement between the computation results obtained using the new method and the classical transient analysis was also obtained for a higher value of load resistance. An increase in frequency causes an increase in the average value of the junction temperature and a decrease in the peak-to-peak value of this temperature.

4.2. Analyses of Properties of the Considered Networks

Using the proposed method, some computations illustrating the influence of the used cooling system, switching frequency and load resistance of the tested networks were performed. Selected results of these computations are presented in Figures 7–14.

Figures 7–11 show the steady-state characteristics of a transistor switch, and Figures 12–14 show a boost converter. The investigations were performed for the SIC-MOSFET situated in different cooling systems. The calculations, the results of which are shown in Figure 7, were made with load resistance R_0 = 40 Ω.

As can be seen in Figure 7a, an increase in frequency causes a practically linear increase in the value of the average power dissipated in the transistor. This increase results from an increase in the switching losses at practically constant conduction losses. In the considered change in frequency from 1 to 400 kHz, the value of p_{avg} increases by up to 10 times. It is also visible that the transistor cooling system has practically no effect on the $p_{avg}(f)$ course. The choice of the cooling system only affects the maximum allowable operating frequency of the circuit under consideration.

An excess in the junction temperature above the ambient temperature ΔT_j is also a linearly increasing function of frequency. The value of this excess for the fixed frequency is proportional to the value of thermal resistance R_{th}. It can be seen that for system A already at frequency f = 100 kHz, the temperature excess ΔT_j reaches 190 K, while for system C at f = 400 kHz, this increase is much smaller and it does not exceed 10 K.

In Figure 7c it can be observed that the peak-to-peak value of the considered temperature excess ΔT_{jpp} is a decreasing function of frequency, and the highest values are obtained for system B characterized by the thermal time constant of the lowest value.

Figure 8 shows the waveforms of the power dissipated in the transistor cooperating with system C and working in the switch circuit loaded with a resistor of R_0 = 40 Ω.

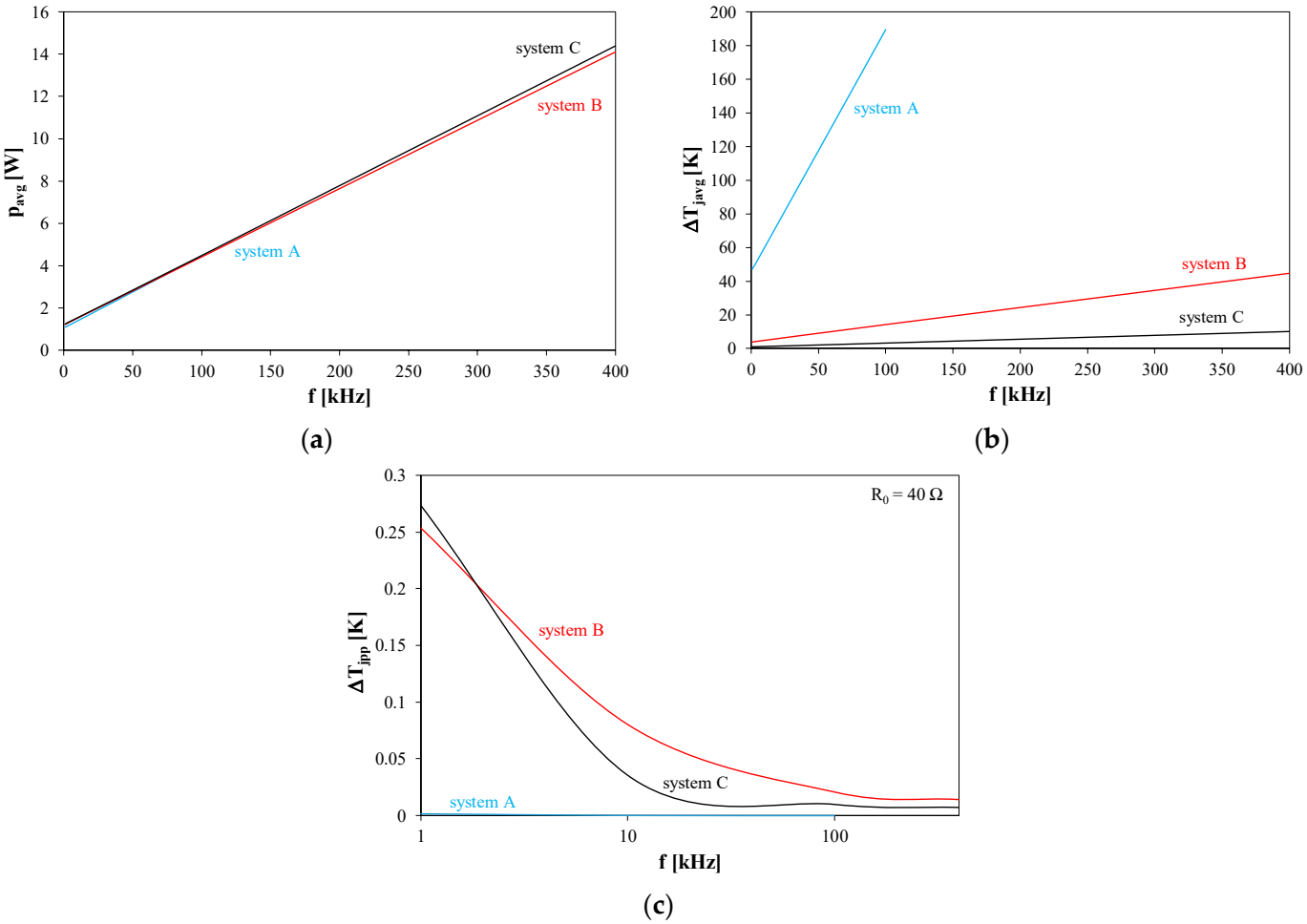

Figure 7. Dependence of the average power value (**a**), of the junction temperature excess (**b**) and the peak-to-peak value of the junction temperature ripples (**c**) on frequency for the transistor operating in the switch circuit cooperating with various cooling systems.

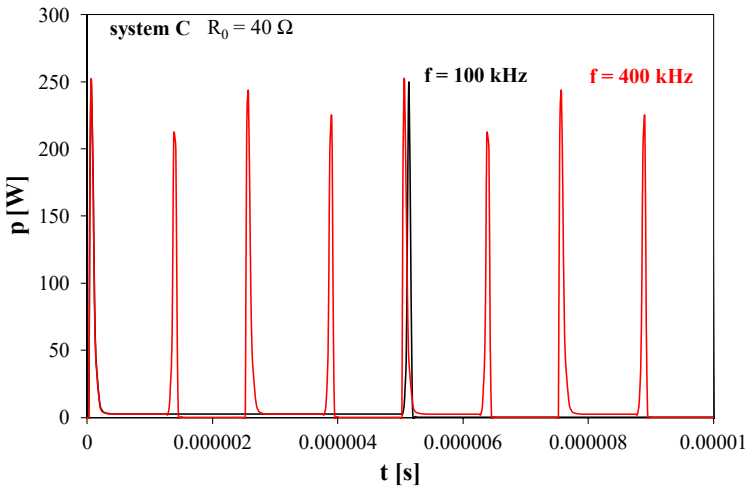

Figure 8. Waveforms of the power dissipated at the steady state in the transistor operating in the switch circuit and cooperating with the cooling system C at selected frequency values.

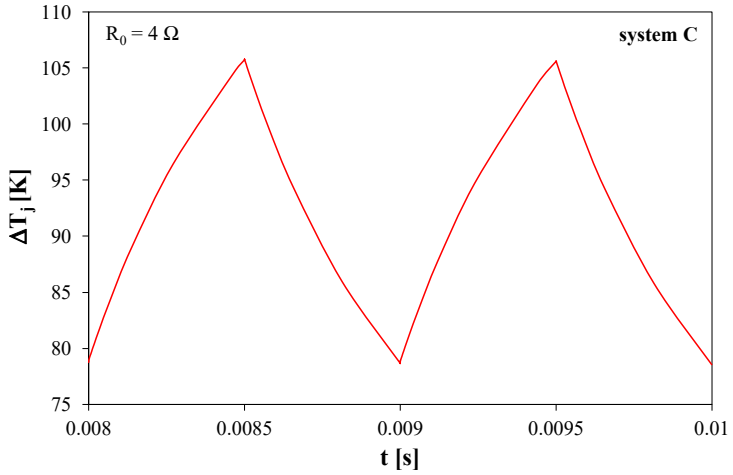

Figure 9. Waveform of the junction temperature at the steady state for the transistor operating in the switch circuit and cooperating with the cooling system C at frequency f = 1 kHz and load resistance R_0 = 4 Ω.

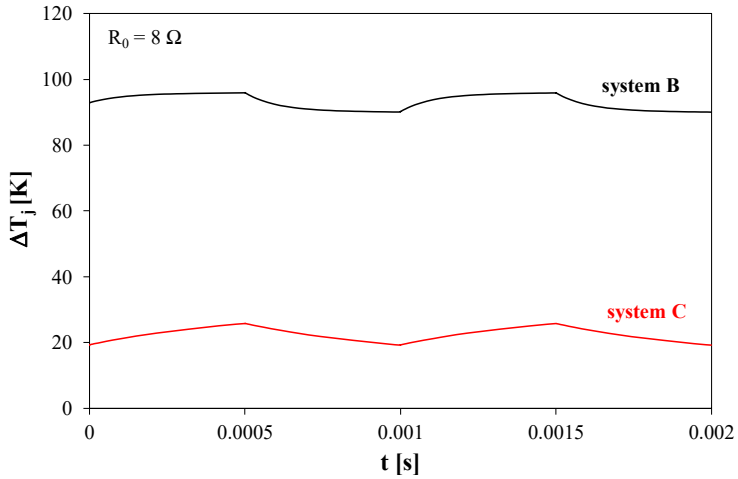

Figure 10. Waveforms of the junction temperature at the steady state for the transistor operating in the switch circuit and cooperating with the cooling systems B and C at frequency f = 1 kHz and load resistance R_0 = 8 Ω.

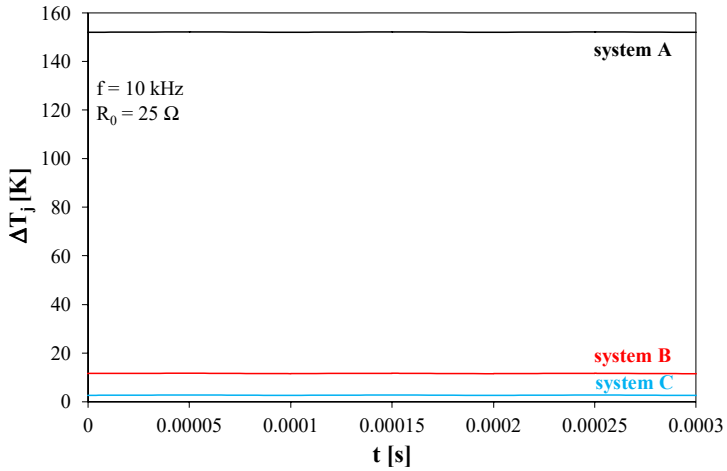

Figure 11. Waveforms of the junction temperature at the steady state for the transistor operating in the switch circuit and cooperating with all the considered cooling systems at frequency f = 10 kHz and load resistance R_0 = 25 Ω.

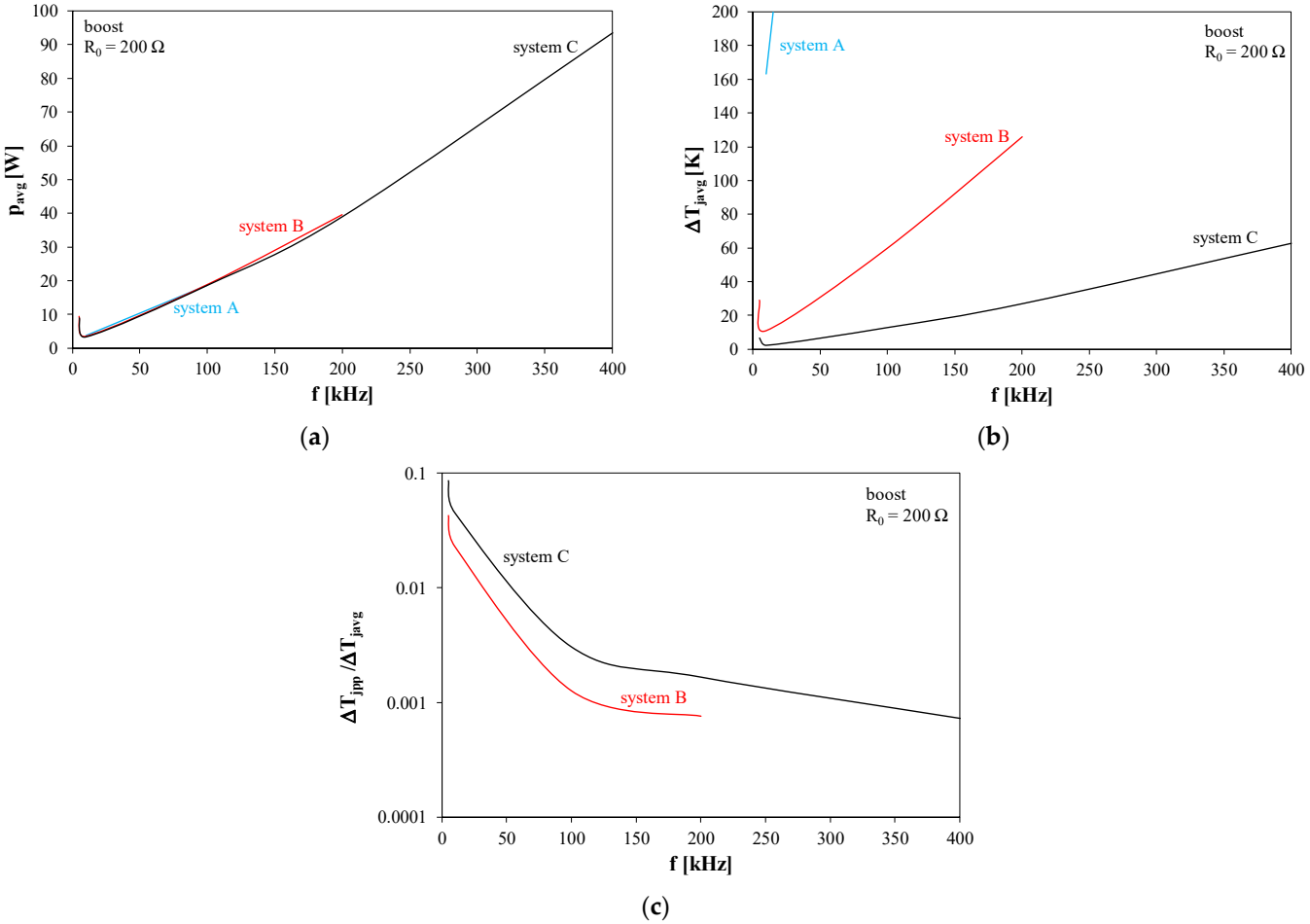

Figure 12. Dependence of the average power value (**a**), the excess of the junction temperature (**b**) and the quotient of the peak-to-peak value of ripples to the average value of the junction temperature (**c**) on frequency for the transistor operating in the boost converter and cooperating with different cooling systems.

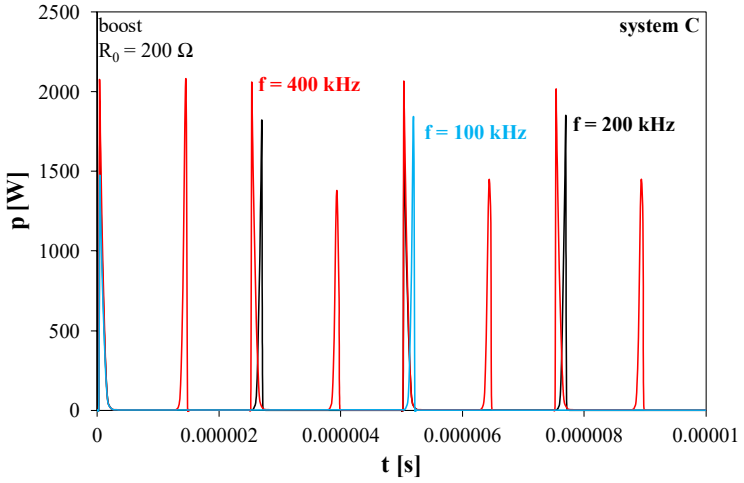

Figure 13. Waveforms of the power dissipated at the steady state in the transistor operating in the boost converter and cooperating with system C at selected frequency values.

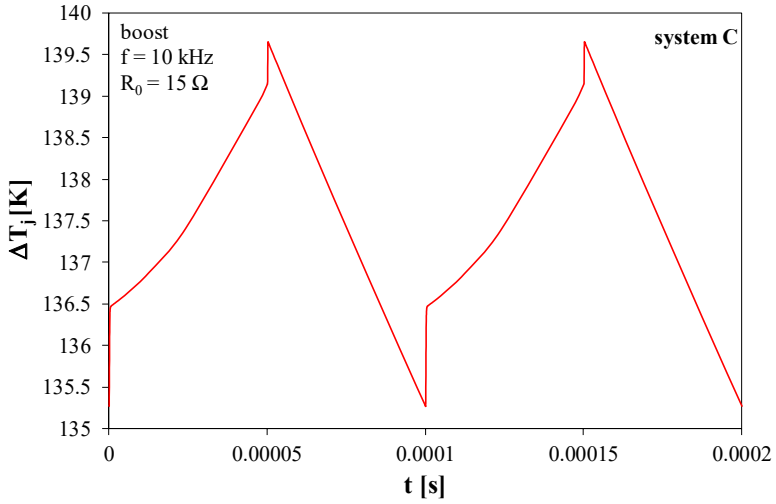

Figure 14. Waveform of the junction temperature at the steady state for the transistor working in the boost converter and cooperating with the cooling system C at frequency f = 10 kHz and load resistance R_0 = 15 Ω.

You can clearly see that there are large bursts of the power dissipated in the transistor when it is turned on and off. With an increase in the operating frequency of the switch, the average value of the power dissipated increases due to an increase in the number of power pulses per time unit. It is worth noting that the power dissipated in the transistor when it is turned on (conduction losses) is even a hundred times lower than the maximum power dissipated during the transistor switching. The presented $p(t)$ waveforms justify the increasing dependence of the average value of power p_{avg} on the frequency observed in Figure 7a.

The peak-to-peak values of temperature excess ΔT_{jpp} obtained with load resistance R_0 = 40 Ω are low. In order to check the influence of load resistance on this temperature excess, some analyses of the considered system were carried out at other values of R_0. Figure 9 shows the steady state $\Delta T_j(t)$ waveforms computed for the system operating at frequency f = 1 kHz, loaded with the resistor of R_0 = 4 Ω and cooperating with the cooling system C.

As can be seen, under the considered operating conditions, the transistor junction temperature ripple is characterized by the peak-to-peak value of as much as 27 K. This means that the peak-to-peak value corresponds to as much as 30% of the average value of this temperature excess. For the other cooling systems under the considered cooling conditions, the junction temperature exceeds the maximum allowable value for the transistor under consideration.

Figure 10 shows the results of calculations of the waveforms of the junction temperature excess of the transistor operating in the switch circuit operating at frequency f = 1 kHz and load resistance R_0 = 8 Ω.

It can be seen that the shape of the $\Delta T_j(t)$ waveforms is significantly different for both the cooling systems under consideration. The observed differences result from the strong differentiation of the thermal values of time constants in system B and small differences in the values of these parameters for system C. The peak-to-peak values of the junction temperature excess ΔT_j reach up to 7 K.

Figure 11 presents the waveforms of ΔT_j obtained at frequency f = 10 kHz and load resistance R_0 = 25 Ω for all the considered cooling systems.

As is visible, the obtained waveforms $\Delta T_j(t)$ are nearly constant functions. The values of ΔT_j change between 2 K for system C and 155 K for system A. The peak-to-peak value of the junction temperature changes from 1 mK for system A to 0.168 K for system B and is much lower than the average value of this temperature at the steady state.

Figure 12 shows the influence of frequency on the average value of the power dissipated in the transistor working in the boost converter (Figure 12a), the average value of the internal temperature excess of this transistor ΔT_{javg} (Figure 12b) and the quotient of the peak-to-peak value to the average value of this temperature excess (Figure 12c). The calculations were performed with the load resistance of the converter equal to 200 Ω and the operating frequency f in the range from 10 to 400 kHz. The value of the output voltage of the converter in these operating conditions is in the range from 408 to 435 V. This means that the power dissipated in the load is in the range from 832 W to 946 W.

As can be seen, the shape of the dependences presented in Figure 12 is the same as the analogous relations presented in Figure 7. It is worth noting, however, that in the case of the boost converter, an increase in frequency causes much lower changes in the average power value and an increase in the junction temperature of the power MOSFET. It can also be seen that under the considered operating conditions, already at frequency f = 10 kHz and the cooling system A, the junction temperature of the transistor reaches a value close to the maximum allowable value given by the manufacturer. On the other hand, an increase in frequency to 400 kHz causes an increase by more than twenty-fold in the value of the average power dissipated in the transistor. Figure 12c shows that the quotient of the peak-to-peak value of the junction temperature ripple of the transistor and the average value of the junction temperature excess above the ambient temperature is a decreasing function of frequency, and at f = 10 kHz, it can even reach several percent.

Figure 13 shows the waveforms of the power dissipated at the steady state in the transistor included in the boost converter and cooperating with system C. The calculations were made for selected frequency values.

As can be seen, the actual value of the power dissipated in the transistor exceeds 2 kW. At the same time, the value of conduction losses do not exceed 5 W. This means that in the high frequency range of the boost converter, the value of the average power dissipated in the transistor is determined by dynamic losses related to the transistor switching process. They can be up to twenty times bigger than the losses due to the current flowing through the switched transistor in the on-state.

Figure 14 shows the waveform of the junction temperature of the transistor working in the boost converter, determined at frequency f = 10 kHz and resistance R_0 = 15 Ω. The presented results concern the transistor cooperating with system C.

As can be seen, under the considered operating conditions, ripples of the junction temperature of the transistor are visible, and their peak-to-peak value exceeds 4 K.

5. Conclusions

This paper describes a new method of computing the waveforms of the junction temperature of discrete power SiC-MOSFETs operating in switched networks at the steady state. It is proved that this method makes it possible to obtain the correct results at a much shorter computation time than for the classical method of transient analysis. On the other hand, the use of the method using one non-physical thermal time constant makes it possible to obtain the correct average value of the junction temperature at the steady state, but the peak-to-peak value of this temperature can be much underestimated. It is worth emphasizing that in the electrothermal analysis of switching circuits, the power of switching losses should not be ignored as this may lead to a significant underestimation of the junction temperature.

For two typical applications of power electronic networks some electrothermal computations were performed for different cooling systems of the transistor. The classical switch with a power SiC-MOSFET and a boost converter with this transistor were considered.

The computer simulations show that switching losses in the transistor are an important component of power losses. Their part in the total losses is an increasing function of switching frequency and can be as high as 95%. As the switching frequency increases, the junction temperature T_j of the transistor also increases in proportion to the value of thermal resistance. The variable wave of the power dissipated in the transistor causes ripples in

the $T_j(t)$ waveform. The peak-to-peak value of these ripples depends on the switching frequency, load resistance and transient thermal impedance of the transistor characterizing the dynamic properties of the cooling system used. The peak-to-peak value of temperature T_j ripples is a decreasing function of frequency and load resistance. The considered ripples are the biggest for system C with very short thermal time constants. If the period of the transistor control signal is close to the values of thermal time constants, the peak-to-peak values of ripples of the transistor junction temperature may exceed even 25 K. If this period is bigger, these ripples can be much bigger.

The observed peak-to-peak values of the transistor junction temperature ripples may affect the reliability of such transistors. For example, at very low switching frequency and a high value of the dissipated power, the value of the junction temperature can change between the room temperature and the welding temperature of the soldering alloy. Such an operation mode can result in a very short lifetime of the used transistor. It is worth noting that these ripples are the biggest for the system, in which the most effective cooling system of the transistor case is used, while the peak-to-peak value of these ripples is negligible for the classical passive transistor cooling systems characterized by a high value of thermal resistance and long thermal time constants.

The presented investigation results may be useful for designers of cooling systems for transistors working in power supply systems. They show that the indispensable efficiency of a cooling system depends strongly on the operating frequency of the analyzed circuit. On the other hand, it is also important that for cooling systems characterized by longer thermal time constants it is possible to obtain a lower smaller peak-to-peak value of the transistor junction temperature. Therefore, free cooling systems could be better than forced cooling systems for power transistors operating in switching circuits. The obtained results will also be used to develop more accurate and faster methods of the electrothermal analysis of switching circuits.

Author Contributions: Conceptualization, K.G.; methodology, K.G. and P.G.; validation, K.G. and P.G.; investigation, K.G.; writing—original draft preparation, K.G. and P.G.; writing—review and editing, K.G. and P.G.; visualization, K.G. and P.G.; supervision, K.G. All authors have read and agreed to the published version of the manuscript.

Funding: The project is financed within the program of the Ministry of Science and Higher Education called "Regionalna Inicjatywa Doskonałości" in the years 2019–2022, the project number 006/RID/2018/19 and the sum of financing 11 870 000 PLN.

Institutional Review Board Statement: Not applicable.

Informed Consent Statement: Not applicable.

Data Availability Statement: Data available on request.

Conflicts of Interest: The authors declare no conflict of interest.

References

1. Perret, R. *Power Electronics Semiconductor Devices*; John Wiley & Sons: Hoboken, NJ, USA, 2009.
2. Rashid, M.H. *Power Electronic Handbook*; Academic Press: Cambridge, MA, USA; Elsevier: Amsterdam, The Netherlands, 2007.
3. Kazimierczuk, M.K. *Pulse-width Modulated DC-DC Power Converters*; John Wiley &Sons, Ltd.: Hoboken, NJ, USA, 2008.
4. Górecki, P.; Górecki, K. Methods of Fast Analysis of DC-DC Converters—A Review. *Electronics* **2021**, *10*, 2920. [CrossRef]
5. Schweitzer, D.; Ender, F.; Hantos, G.; Szabo, P.G. Thermal transient characterization of semiconductor devices with multiple heat-sources—Fundamentals for a new thermal standard. *Microelectron. J.* **2015**, *46*, 174–182. [CrossRef]
6. Blackburn, D.L. Temperature measurements of semiconductor devices—A review. In Proceedings of the Twentieth Annual IEEE Semiconductor Thermal Measurement and Management Symposium, San Jose, CA, USA, 11 March 2004; pp. 70–80.
7. Bagnoli, P.E.; Casarosa, C.; Ciampi, M.; Dallago, E. Thermal resistance analysis by induced transient (TRAIT) method for power electronic devices thermal characterization. *IEEE Trans. Power Electron. I Fundam. Theory* **1998**, *13*, 1208–1219. [CrossRef]
8. Górecki, P.; Wojciechowski, D. Accurate Computation of IGBT Junction Temperature in PLECS. *IEEE Trans. Electron Dev.* **2020**, *67*, 2865–2871. [CrossRef]
9. Dupont, L.; Avenas, Y.; Jeannin, P.O. Comparison of Junction Temperature Evaluations in a Power IGBT Module Using an IR Camera and Three Thermosensitive Electrical Parameters. *IEEE Trans. Ind. Appl.* **2013**, *49*, 1599–1608. [CrossRef]

10. Bryant, A.; Parker-Allotey, N.A.; Hamilton, D.; Swan, I.; Mawby, P.A.; Ueta, T.; Nishijima, T.; Hamada, K. A Fast Loss and Temperature Simulation Method for Power Converters, Part I: Electrothermal Modeling and Validation. *IEEE Trans. Power Electron.* **2012**, *27*, 248–257. [CrossRef]
11. Ceccarelli, L.; Kotecha, R.; Iannuzzo, F.; Mantooth, A. Fast Electro-thermal Simulation Strategy for SiC MOSFETs Based on Power Loss Mapping. In Proceedings of the 2018 IEEE International Power Electronics and Application Conference and Exposition (PEAC), Shenzhen, China, 4–7 November 2018.
12. Górecki, K.; Zarębski, J.; Górecki, P. Influence of Thermal Phenomena on the Characteristics of Selected Electronics Networks. *Energies* **2021**, *14*, 4750. [CrossRef]
13. Swan, I.; Bryant, A.; Mawby, P.A.; Ueta, T.; Nishijima, T.; Hamada, K. A Fast Loss and Temperature Simulation Method for Power Converters, Part II: 3-D Thermal Model of Power Module. *IEEE Tran. Power Electron.* **2012**, *27*, 258–268. [CrossRef]
14. Langbauer, T.; Mentin, C.; Rindler, M.; Vollmaier, F.; Connaughton, A.; Krischan, K. Closing the Loop between Circuit and Thermal Simulation: A System Level Co-Simulation for Loss Related Electro-Thermal Interactions. In Proceedings of the 2019 25th International Workshop on Thermal Investigations of ICs and Systems (THERMINIC), Lecco, Italy, 25–27 September 2019.
15. Ceccarelli, L.; Bahman, A.S.; Iannuzzo, F.; Blaabjerg, F. A Fast Electro-Thermal Co-Simulation Modeling Approach for SiC Power MOSFETs. In Proceedings of the 2017 IEEE Applied Power Electronics Conference and Exposition (APEC), Tampa, FL, USA, 26–30 March 2017.
16. Szekely, V. A new evaluation method of thermal transient measurement results. *Microelectr. J.* **1997**, *28*, 277–292. [CrossRef]
17. Górecki, K.; Zarębski, J.; Górecki, P.; Ptak, P. Compact thermal models of semiconductor devices—A review. *Int. J. Electron. Telecommun.* **2019**, *65*, 151–158.
18. Górecki, K.; Posobkiewicz, K. Selected problems of power MOSFETs thermal parameters measurements. *Energies* **2021**, *14*, 8353. [CrossRef]
19. Górecki, K.; Zarębski, J. The Method of a Fast Electrothermal Transient Analysis of Single-Inductance DC–DC Converters. *IEEE Trans. Power Electron.* **2012**, *27*, 4005–4012. [CrossRef]
20. Górecki, P.; Górecki, K. Analysis of the Usefulness Range of the Averaged Electrothermal Model of a Diode-Transistor Switch to Compute the Characteristics of the Boost Converter. *Energies* **2021**, *14*, 154. [CrossRef]
21. Pietrenko, W.; Janke, W. Design and simulation of PWM Switch-mode Power Converters. *Bull. Pol. Acad. Sci. Tech. Sci.* **1999**, *47*, 291–300.
22. Górecki, P.; Górecki, K.; Kisiel, R.; Brzozowski, E.; Bar, J.; Guziewicz, M. Investigations of an influence of the assembling method of the die to the case on thermal parameters of IGBTs. *IEEE Trans. Compon. Packag. Manuf. Technol.* **2021**, *11*, 1988–1996. [CrossRef]
23. Ciappa, M.; Carbognami, F.; Cora, P.; Fichtner, W. A novel thermomechanics-based lifetime prediction model for cycle fatigue failure mechnisms in power semiconductors. *Microelectron. Reliab.* **2002**, *42*, 1653–1658. [CrossRef]
24. Górecki, P.; Górecki, K. Measurements and computations of internal temperatures of the IGBT and the diode situated in the common case. *Electronics* **2021**, *10*, 210. [CrossRef]
25. Górecki, K.; Detka, K. Application of Average Electrothermal Models in the SPICE-Aided Analysis of Boost Converters. *IEEE Trans. Ind. Electron.* **2019**, *66*, 2746–2755. [CrossRef]
26. Castellazzi, A.; Kraus, R.; Seliger, N.; Schmitt-Landsiedel, D. Reliability analysis of power MOSFET's with the help of compact models and circuit simulation. *Microelectr. Reliab.* **2002**, *42*, 1605–1610. [CrossRef]
27. Mantooth, H.A.; Peng, K.; Santi, E.; Hudgins, J.L. Modeling of Wide Bandgap Power Semiconductor Devices—Part I. *IEEE Trans. Electron Dev.* **2015**, *62*, 423–433. [CrossRef]
28. Hazra, S.; De, A.; Cheng, L.; Palmour, J.; Schupbach, M.; Hull, B.A.; Allen, S.; Bhattacharya, S. High Switching Performance of 1700-V, 50-A SiC Power MOSFET Over Si IGBT/BiMOSFET for Advanced Power Conversion Applications. *IEEE Trans. Power Electron.* **2016**, *31*, 4742–4754.
29. Zhang, L.; Yuan, X.; Wu, X.; Shi, C.; Zhang, J.Z.Y. Performance Evaluation of High-Power SiC MOSFET Modules in Comparison to Si IGBT Modules. *IEEE Trans. Power Electron.* **2019**, *34*, 1181–1196. [CrossRef]
30. Scognamillo, C.; Catalano, A.P.; Riccio, M.; d'Alessandro, V.; Codecasa, L.; Borghese, A.; Tripathi, R.N.; Castellazzi, A.; Breglio, G.; Irace, A. Compact Modeling of a 3.3 kV SiC MOSFET Power Module for Detailed Circuit-Level Electrothermal Simulations Including Parasitics. *Energies* **2021**, *14*, 4683. [CrossRef]
31. Semiconductor, R.O.H.M. SCT3060AL N-Channel SiC Power MOSFET, 2015. Data Sheet. Available online: www.rohm.com (accessed on 1 September 2022).
32. Semiconductor, R.O.H.M. SCT3060ALHR SPICE Model. Available online: https://www.rohm.com/products/sic-power-devices/sic-mosfet/sct3060alhr-product#technicalAricleSubMenu (accessed on 8 August 2022).
33. IR2125 Current Limiting Single Channel Driver, Infineon Technologies, Data Sheet No. PD60017 Rev.Q, 2004. Available online: https://www.infineon.com/dgdl/Infineon-IR2125-DS-v01_00-EN.pdf?fileId=5546d462533600a4015355c85ba31694 (accessed on 1 September 2022).
34. Górecki, K.; Posobkiewicz, K. Influence of a Cooling System on Power MOSFETs' Thermal Parameters. *Energies* **2022**, *15*, 2923. [CrossRef]